Int. J. Electrochem. Sci., 15 **(2020)** 6748 – 6758, doi: 10.20964/2020.07.69

International Journal of ELECTROCHEMICAL SCIENCE
www.electrochemsci.org

Electrochemical Sensor Based on Aluminum Tetraaminophthalocyanine and Ionic Liquid Modified Glassy Carbon Electrode for Dopamine Detection in Drugs and Human Serum

Weijie Jiao[1], *Cuijie Nong*[2], *Xiaokun Li*[2,*], *Suxiang Feng*[2], *Xuefang Liu*[2]

[1] Department of Pharmacy, Henan Province Hospital of Traditional Chinese Medicine, The Second Affiliated Hospital of Henan University of traditional Chinese Medicine, Zhengzhou, 450002, Henan Province, China.
[2] School of Pharmacy, Henan University of Traditional Chinese Medicine, Zhengzhou 450046, China
[*]E-mail: li96052122@126.com

Received: 2 March 2020 / *Accepted:* 30 April 2020 / *Published:* 10 June 2020

In this work, a novel electrochemical sensor for dopamine (DA) detection was designed based on aluminum tetraaminophthalocyanine-ionic liquid (AlTAPc-IL) composite material. The morphologies and structures of the aluminum tetraaminophthalocyanine (AlTAPc) and AlTAPc-IL materials were characterized by scanning electron microscopy (SEM) and ultraviolet-visible (UV-Vis) spectroscopy. The cyclic voltammetry (CV) and differential pulse (DPV) methods were used to study the electrochemical behaviors of dopamine on the tetraamino AlTAPc-IL/GCE electrode. The results showed that the modified electrode has a higher response signal than the bare electrode. In a phosphate buffer solution (PBS) at pH 7.0, the AlTAPc-IL/GCE electrode has good catalytic activity for the oxidation of DA. The peak current increased linearly with DA concentration in the ranges of 0.1-30 μM and 30-500 μM with good correlation coefficients, and the detection limit was 0.38 nM. Due to its high sensitivity, low detection limit and wide linear range, the sensor can be used as an alternative analytical tool for the detection of dopamine in actual samples.

Keywords: Aluminum tetraaminophthalocyanine, Ionic liquid, Dopamine

1. INTRODUCTION

Dopamine (3,4-dihydroxyphenylethylamine, DA) is an important neurotransmitter in the central nervous system of mammals and plays a very important role in central regulatory function [1,2]. The dose of DA has an important effect on the human body and must be strictly controlled, with abnormal DA levels giving rise to a variety of diseases such as schizophrenia, Huntington's disease and Parkinson's disease, and HIV infection [3,4]. Therefore, determination of the DA content in pharmaceutical

preparations is essential for basic research and early diagnosis [5]. DA detection has been carried out by a number of methods such as fluorescence spectroscopy [6,7], chemiluminescence analysis [8,9], high-performance liquid chromatography [10,11], colorimetry [12,13], and photoelectrochemical analysis [14,15]. Compared with the above methods, electrochemical analysis technology is favored by researchers because of its simple operation, high sensitivity, fast response speed, and cheap instruments.

Metal phthalocyanine (MPc) compounds are important tetrapyrrole derivatives with a widely delocalized 18π aromatic conjugated system and stable chemical properties [16,17]. In recent years, metal phthalocyanines and functionalized phthalocyanines have been widely used due to their excellent chemical and physical properties such as thermal stability, chemical inertness, photoconductivity and semiconductivity, and suitability for acting as electron donors and electron acceptors [18-22]. These compounds have been used in many technical fields include chemical sensors [23], energy conversion (photovoltaic and solar cells) [24], gas sensors [25], photodynamic therapy [26], catalysis [27], and nonlinear optics [28]. In addition, functional groups can be introduced into metal phthalocyanines to improve their performance and overcome some of their shortcomings. These functional groups include nitro, amino, and carboxyl groups, [29,30]. For example, the performance of tetraaminophthalocyanine (MTAPC) is significantly better than that of MPC, and it can be dissolved in some organic solvents, and has been widely used in the field of electrochemistry [18]. Ionic liquids (ILs) are organic salts or a mixture of salts containing organic cations and various anions [31,32]. Because of their unique physical and chemical properties, such as high ionic conductivity, wide electrochemical window, negligible vapor pressure, good chemical and thermal stability, and good antifouling ability, ILs have been widely used in the field of electrochemistry [33-36].

In this study, an electrochemical sensor for DA detection was developed based on an aluminum tetraaminophthalocyanine and ionic liquid (AlTAPc-IL) composite material. The electrochemical characterization of the AlTAPc-IL/GCE electrode was performed by electrochemical impedance spectroscopy (EIS) and chronocoulometry (CC). The electrochemical behaviors of DA on the AlTAPc-IL/GCE electrode were studied by cyclic voltammetry (CV) and the differential pulse method (DPV). The experimental results show that the developed sensor has high conductivity, high sensitivity, good selectivity, and low detection limit, and can be used for real sample detection.

2 EXPERIMENTAL SECTION

2.1 Instruments

A CHI 760E electrochemical workstation (Shanghai Chenhua Instrument Co., Ltd., China) was used for electrochemical experiments. The electrochemical workstation was directly connected to a three-electrode battery system. An AlTAPc-IL/GCE electrode was used as the working electrode. A Pt line was used as the auxiliary electrode, and a saturated Ag/AgCl was used as the reference electrode. The size and morphology of the experimental materials were characterized by scanning electron microscopy (SEM) (Hitachi S-4800, Tokyo, Japan; 5 kV). An ultraviolet-visible (UV-Vis) spectrophotometer (UV 6100S, Metash, Shanghai, China) was used to analyze the structure of the materials. The pH of the solution was measured using a pH meter (pHS) (3C, Rex, Shanghai, China).

2.2 Chemicals and materials

Aluminum chloride, sodium sulfate, and ammonium molybdate were obtained from Xilong Science Co., Ltd. (Guangdong, China). N,N-dimethylformamide (DMF) and other chemicals were purchased from Chengdu Kelong Chemical Reagent Factory (Chengdu, China). DA was purchased from Aladdin Biochemical Technology Co., Ltd. (Shanghai, China). All of the reagents used in this study were of analytical grade. A phosphate buffer solution (PBS, 0.2 M) was prepared with disodium hydrogen phosphate and sodium dihydrogen phosphate. A 0.2 M HCl solution and a 0.2 M NaOH solution were used to adjust the pH of the buffer solution. The solutions used in the experiments were prepared using distilled water. Human serum samples were provided from the Chongzuo People's hospital (Chongzuo, Guangxi, China). All of the experiments were performed in accordance with the National Law and Regulations of the Committee of Related Institutions.

2.3 Synthesis of AlTAPc

The AlTAPc material was prepared following the methods reported in the literature [18]. Typically, 4-nitrophthalimide (8.50 g), urea (20.10 g) and ammonium molybdate (0.10 g) were ground in a mortar, and then were transferred to a flask and heated. After the mixture was melted, aluminum trichloride (2.04 g) was added, and the temperature was maintained at 180°C. The reaction was stopped when the reactants no longer swell, and a blue-violet solid was obtained. The obtained solid product was boiled with an HCl solution (1 M, 300 mL) for 1 h, filtered by suction and washed with distilled water. Then, the solid product was placed into a NaOH solution (1 M, 300 mL) and boiled for 1 h, and the solid product was filtered by suction and washed with distilled water. After drying, aluminum tetranitrophthalocyanine was obtained. Aluminum tetranitrophthalocyanine (0.75 g), $Na_2S·9H_2O$ (2.88 g), and DMF (50 mL) were added into a 250 mL three-necked flask to carry out the reflux reaction, and the temperature was maintained at 60°C for 1 h. Then, the synthesized product was treated with distilled water (150 mL) to obtain AlTAPc.

2.4 Preparation of modified electrodes

Initially, the bare glassy carbon electrode (GCE) was washed with double distilled water on an aluminum polishing cloth pad with a 0.5 μm alumina slurry, then was washed with pure water, and finally was dried at room temperature. AlTAPc (2 mg) and IL (40 μL, 0.5 mg/mL in DMF) were added to DMF (1 mL). A uniform modification solution was obtained by ultrasonication for 30 minutes. Then, the modifier (6 μL) was dropped on the GCE to obtain AlTAPc-IL/GCE. The modified electrode was dried under irradiation provided by an infrared lamp. For comparison, AlTAPc- and IL-modified GCEs were respectively prepared using the method described above. All of the electrochemical tests were performed at room temperature.

3. RESULTS AND DISCUSSION

3.1 Characterization of materials

The AlTAPc and AlTAPc-IL materials were separately dispersed in the DMF solution. The morphology of AlTAPc-IL was studied by SEM. SEM images of AlTAPc and AlTAPc-IL materials are shown in Figs. 1A and 1B. It is observed from Fig. 1A that the shape of AlTAPc is irregular and shows no specific morphological characteristics. In the SEM image of AlTAPc-IL/GCE, AlTAPc was uniformly dispersed on the surface of GCE after the addition of ILs to form the AlTAPc-IL material, and specific morphological characteristics can be observed, indicating that the AlTAPc-IL composite has been successfully formed.

The UV-Vis spectra of AlTAPc and AlTAPc-IL are shown in Fig. 1C. Phthalocyanine and its derivatives have two characteristic absorption peaks known as the B-band and the Q-band. The band (Q band) in the 600-750 nm range is due to the allowed π-π transition of phthalocyanine [33]. AlTAPc showed absorption peaks at 341 nm^{-1} and 740 nm^{-1}, as shown in Fig. 1C (curve a). On the other hand, as shown in Fig. 1C (curve b), the Q-band of AlTAPc-IL was shifted significantly toward shorter wavelengths. This may be due to the diffusion of the π electrons of AlTAPc to IL, resulting in a blueshift of the AlTAPc energy band, providing an additional confirmation for the formation of the AlTAPc-IL composite.

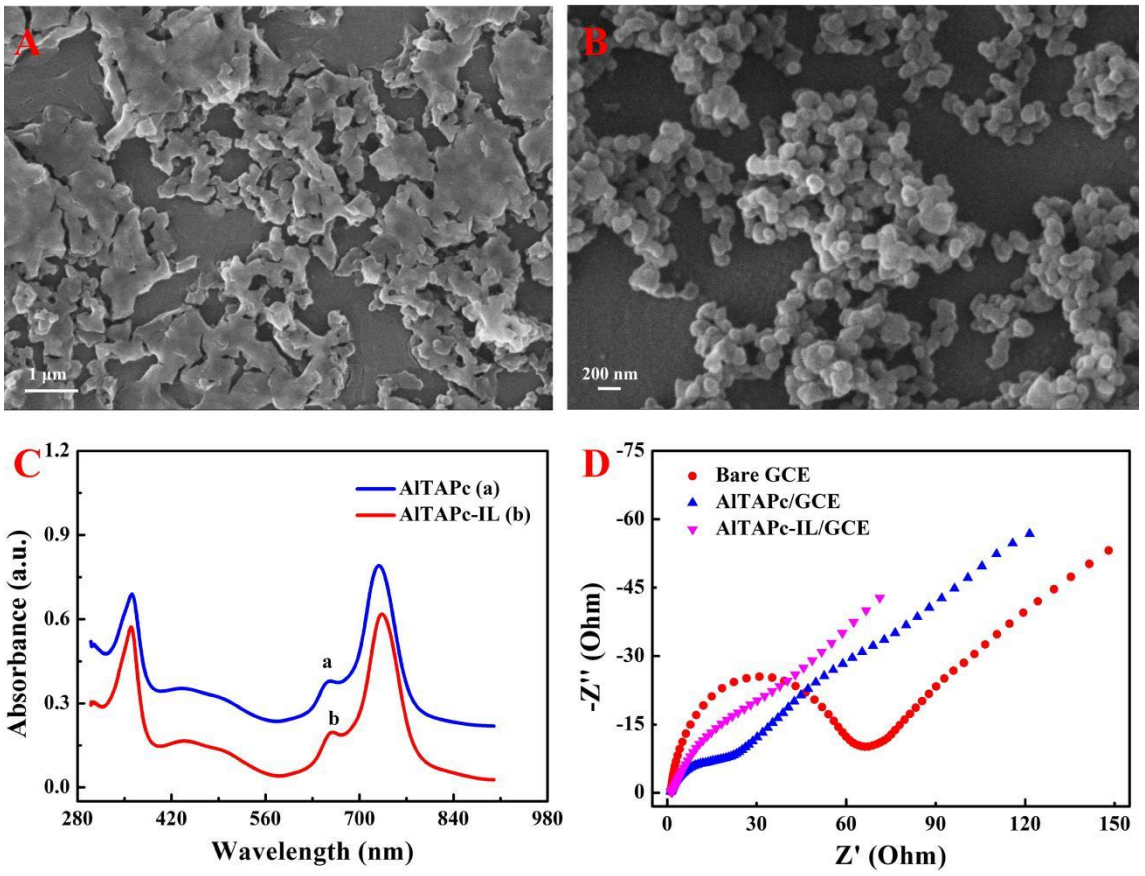

Figure 1. SEM images of (A) AlTAPc and (B) AlTAPc-IL. (C) UV-Vis spectra of AlTAPc and AlTAPc-IL. (D) Electrochemical impedance plots of different electrodes.

3.2 Electrochemical impedance spectroscopy

Electrochemical impedance spectroscopy (EIS) was used to explore modified electrodes. The charge transfer behavior of the GCE and AlTAPc-IL/GCE electrodes was studied in a 2.0 mM $K_3[Fe(CN)_6]/K_4[Fe(CN)_6$ solution containing 0.1 M KCl. The semicircle at high frequencies is due in part to the charge transfer resistance (Rct) in the EIS, and reflects the electron transfer capability of the electrode. The radius of the semicircle corresponds to this resistance [32]. As shown in Fig. 1D, compared with the modified electrode, the diameter of the semicircle of the GCE electrode was larger. The results showed that the Rct of the modified electrode is lower than that of the GCE electrode. This is because the electrocatalytic activity of the AlTAPc material and the high conductivity of IL increased the electron transfer rate of AlTAPc-IL/GCE, and accelerated the electron transfer between the electrolyte and the electrode surface[37].

3.3 Electrochemical behavior of DA on different modified electrodes

The electrochemical behavior of DA on different electrodes was examined in a PBS solution at pH 7.0. As shown in Fig. 2A, in the absence of DA, the response signal of the bare GCE (curve a) was 81.4 nA and the response signal of AlTAPc-IL/GCE (curve b) was 210 nA. It is clear that the response signal of AlTAPc-IL/GCE was significantly stronger than response signal of the bare GCE. In the presence of 35 μM DA, compared with the GCE (curve c), when DA was detected using AlTAPc-IL/GCE (curve d), the peak current of DA was significantly increased, and the potential of the oxidation peak was shifted toward the anode. These results showed that the AlTAPc-IL-modified electrode has good catalytic effect and high electrical conductivity.

3.4 Optimize experimental conditions

To identify the optimal electrochemical detection conditions, the material concentration and pH were optimized. In this study, the amount of the introduced AlTAPc (1.0, 1.5, 2.0, and 2.5 mg) and the added IL (20, 30, 40, and 50 μL) were varied. The results showed that in 1 mL of DMF, the strongest GCE current response was obtained using 2.0 mg of AlTAPc and 40 μL of IL, as shown in Fig. 2B. In addition, timed amperometric analysis of DA on AlTAPc-IL/GCE was performed at different pH values in the range of 2.0-9.0 in the PBS solution (Fig. 2C). It was found that the peak current of DA increased gradually with the increasing pH, and reached the maximum value at pH 7.0. Then, the peak current was gradually reduced until pH 9.0. Therefore, subsequent measurements were carried out in the PBS buffer solution at pH 7.0.

3.5 Effect of scan rate

Under the optimal conditions, cyclic voltammetry (CV) was used to study the effect of the scanning speed on the electrochemical behavior of DA on the AlTAPc-IL/GCE electrode. The scanning

speed range was 0.01-1.0 V/s. As shown in Fig. 2D, the peak oxidation current of DA increases with the scanning speed (within the scanning speed range), and the peak current shows a good linear relationship with the scan rate (0.03-1.0 V/s). The linear equation for the scan rate is: $Ipa = 2.20 + 6.311v$ (V/s), and the correlation coefficient is 0.9922. The linear relationship between the peak current and the scan rate indicates that the behavior of the DA on the modified electrode can be characterized as an electrochemical adsorption process. The potential (*Ep*) and the logarithm (lnν) of DA show a linear relationship. The linear equation for this relationship is $Epa = 0.353 + 0.040\ lnv$ (V/s), and the correlation coefficient is 0.9977. The linear relationship between the peak current (Ip) and the scan rate (ν) indicates that DA detection is carried out through adsorption-controlled processes on the target-modified electrode [38].

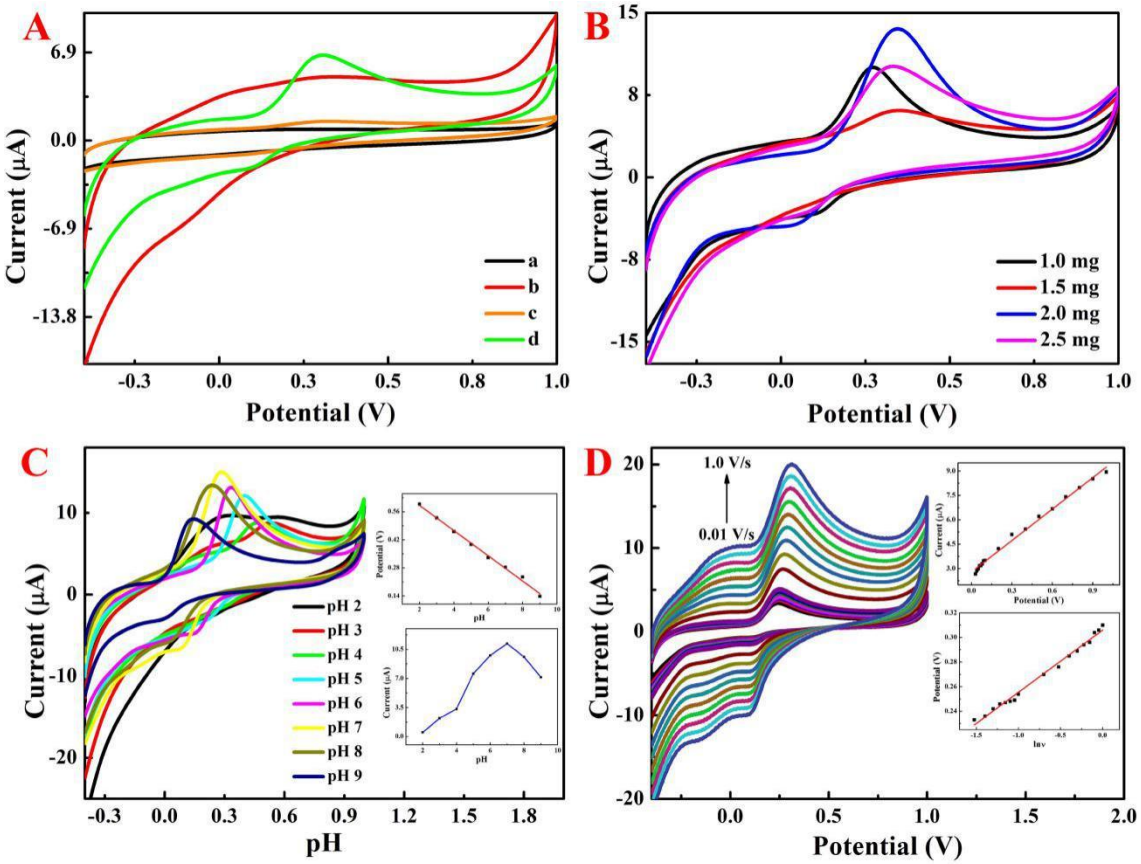

Figure 2. (A) CVs for 35 μM DA at the various electrodes, GCE in the absence (a) and presence of the analyte (c), AlTAPc-IL/GCE in the absence (b) and presence of the analyte (d) in a pH 7.0 PBS solution. (B) CV responses of AlTAPc-IL/GCE at the different concentrations of the modified solution. (C) CV response and its linear relationship at different pH values. (D) CVs of different scan rates at the sweep rate of 0.3-1.0 V/s.

3.6 Studies of the effective surface area

In a 1.0 mM $K_3[Fe(CN)_6]/K_4[Fe(CN)_6$ solution containing 0.1 M KCl, the effective surface area of the bare GCE, IL/GCE, AlTAPc/GCE, and AlTAPc-IL/GCE electrodes were studied by

chronocoulometry. As shown in Fig. 3, the Q-$t^{1/2}$ curve equations for bare/GCE, IL/GCE, AlTAPc/GCE, AlTAPc-IL/GCE are:

$$Q_{\mu C}\,(\text{Bare}) = 20.94t^{1/2} - 1.95\ (R^2 = 0.9989),$$
$$Q_{\mu C}\,(\text{IL}) = 22.04t^{1/2} + 4.09\ (R^2 = 0.9988),$$
$$Q_{\mu C}\,(\text{AlTAPc}) = 259.35t^{1/2} - 10.28\ (R^2 = 0.99581),$$
$$Q_{\mu C}\,(\text{AlTAPc-IL}) = 259.35t^{1/2} - 14.28\ (R^2 = 0.99581).$$

Anson's equation [39] was used to calculate the effective surface area of the bare electrode and AlTAPc-ILGCE. The effective surface area of AlTAPc-IL/GCE was 11.94 times larger than that of bare GCE, showing a significant increase. This shows that the AlTAPc-IL/GCE electrode has a larger relative electrochemical surface area and provides more active site for DA detection [40].

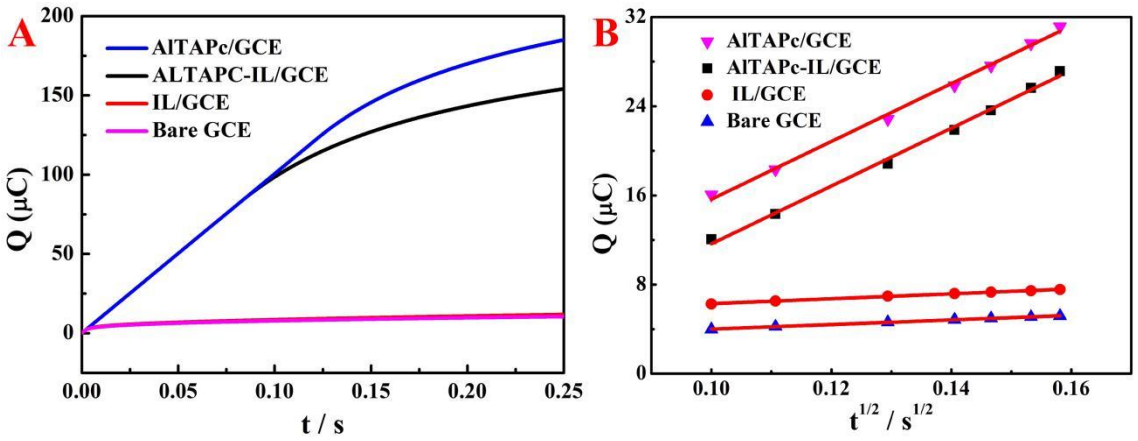

Figure 3. (A) Chronocoulometry curves and (B) the corresponding Q-$t^{1/2}$ plots of the various electrodes in a 1.0 mM $K_3[Fe(CN)_6]/K_4[Fe(CN)_6$ solution containing 0.1 M KCl.

3.7 Differential pulse voltammetric determination for DA

Under optimal conditions, the electrochemical behaviors of DA at different concentrations on AlTAPc-IL/GCE were investigated using differential pulse voltammetry (DPV). As shown in Fig. 4, it was found that the peak current of DA increases with increasing DA concentration. A good piecewise linear relationship was observed for the ranges of 0.1-30 μM and 30-500 μM. The corresponding linear equations (Fig. 4) are I_1 (nA) = 0.012 + 0.046C_{DA} (μM) (R = 0.9987) and I_2 (nA) = 1.29 + 0.0050C_{DA} (R = 0.9974), respectively. The detection limit was 0.38 nM (S/N = 3). At low substrate levels, due to the diffusion effect at the electrode surface, even small changes in the concentration can cause significant changes in the response signal. In addition, at low DA concentration the local concentration decreased rapidly at the electrode surface as the AlTAPc-IL/GCE converted DA into product. In this case, the sensor exhibits high sensitivity. At higher DA levels, the time period of interaction between material and substrate is longer. This together with possibility of fouling the electrode surface by the reaction products, leads to a lower slope. Thus, at high and low concentrations, the sensors showed two linear correlations [41]. In addition, the as-constructed sensor was compared to the reported DA sensors, as shown in Table 1. An examination of the data presented in Table 1 shows that the DA sensor prepared in

this work has a wider linear range and a lower detection limit than the other sensors, indicating that this sensor is highly significant for the quantitative analysis of DA.

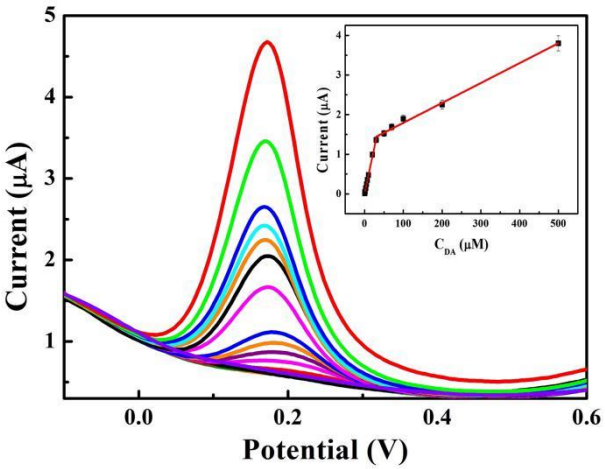

Figure 4. DPVs for detecting DA at AlTAPc-IL/GCE electrode in pH 7.0 PBS. Inset: linear relationship of the reduction peak currents vs. DA concentrations.

Table 1 Comparison of the proposed sensor with other reported sensors used for DA determination

Electrode	Method	Linear rang (μM)	Detection limit (μM)	Refs.
GQDs[a]@MWCNTs[b]/GCE	DPV	0.25-250	0.095	42
Au@ZIF-8[c]/GCE	DPV	0.1-50	0.01	43
(Ce-ZrO_2/CPE[d]	DPV	0.5-10	3.6	44
POMOF[e]/rGO[f]/GCE	DPV	1-200	0.08	45
CuO nanodots-ITO[g]	DPV	0.12-56.87	0.03	46
GQDs-Nafion/GCE	DPV	0.005-100	0.00045	47
N-G[h]/NiTsPc[i]/GCE	DPV	0.1-200	0.1	48
AlTAPc-IL/GCE	DPV	0.1-30; 30-500	0.00038	This work

a) graphene quantum dots; b) multiwall carbon nanotubes; c) zeolitic imidazolate framework-8; d) carbon paste electrode; e) polyoxometalate-based metal-organic framework; f) reduced graphene oxide; g) indium tin oxide-coated glass slide; h) nitrogen-doped graphene; i) nickel tetrasulfonated phthalocyanine

3.8 Stability and repeatability of AlTAPc-IL/GCE

The modified electrode was stored in a refrigerator at 4°C for 7 days. Under optimal conditions, the peak current of the electrode was measured on days 1-7. The stability of the sensor was evaluated by comparing the peak current of DA detected in a standard solution within one week. The relative standard deviation (RSD) obtained was 4.57%, indicating that the AlTAPc-IL/GCE electrode has good stability. The repeatability of the sensor was checked by detecting DA with 7 electrodes prepared in parallel. After seven consecutive measurements, the peak current remained stable and reached 4.4% RSD, proving that

the sensor has good repeatability.

3.9 Interference studies

Interference studies were performed on some common interference substances (such as amino acids, uric acid, ascorbic acid, glucose, sucrose, and metal ions) to explore the selectivity the sensors and their feasibility for practical use. The maximum allowable interference limit was defined as the change in the peak current value of DA at a certain concentration before and after the interference substance was added by less than ±5%. As shown in Table 2, the results showed that the peak current change of these interfering substances is within ±5%, and the peak current of DA was not affected by the interfering substances.

Table 2. Interference study of some species for the simultaneous determination of 0.35 μM of DA

Foreign species	Molar ratio (foreign species/DA)
Ba^{2+}, NO_3^-, Ca^{2+}, Cu^{2+},Al^{3+}, Zn^{2+}, SO_4^{2+}, K^+, $S_2O_3^{2-}$, Br^-, NH_4^+, CO_3^{2-}, Ni^{2+}, Mn^{2+}, Mg^{2+}, Cl^-, CH_3COO^-, Na^+	200
uric acid	100
ascorbic acid	100
maltose	100
oxalic acid, sucrose	100
L-tryptophan, L-arginine, leucine, phenylalanine, phenylalanine	100

3.10 Detection of DA in actual samples

DA content tests were performed in human serum and injection to check the feasibility of the use of the AlTAPc-IL/GCE sensor in clinical sample detection. For human serum samples, the accuracy of the experimental results is expressed in recoveries (Table 3).

Table 3. Results of DA determination in serum samples under optimal conditions.

Sample	Added (μmol/L)	Found (μmol/L)	Recovery (%)	RSD (%, n = 5)
Serum1	15	15.4	103.14	3.7
Serum2	20	20.7	103.78	1.6
Serum3	25	26.6	106.56	1.8

The AlTAPc-IL/GCE electrode shows no current response in human serum, indicating that the electrode can be used to detect DA in human serum. In addition, the content of a commercially available DA injection was measured using high-performance liquid chromatography, and compared with the DA

level measured by an AlTAPc-IL/GCE sensor (Table 4). There were no significant differences between the results obtained by the two techniques. Experimental results show that the sensor has important practical significance for DA detection in actual clinical samples.

Table 4. Results for the DA determination in the drug under the optimal conditions.

Sample	Labeled amount (mg/mL)	Found by HPLC (mg/mL)	Found by DPV (mg/mL)	Percentage of labeled amount (%)	RSD (%, n = 5)
dopamine hydrochloride injection	10	10.41	9.83	98.31	1.56

4 CONCLUSIONS

In this paper, based on the use of aluminum phthalocyanine and ionic liquid (dissolved in DMF), a new sensor for DA detection was prepared based on the AlTAPc-IL/GCE electrode. It was found that the effective specific surface area of the AlTAPc-IL/GCE electrode was larger than that of the bare/GCE electrode and also has better electrocatalytic activity. In addition to its good anti-interference ability to interfering substances, the sensor also has the advantages of simple operation, high conductivity, good stability and repeatability. Furthermore , in this work, the AlTAPc-IL/GCE electrodes were used for the detection of DA in actual samples.

ACKNOWLEDGEMENTS
This work was financially supported by the Key research program of higher education of Henan province (20A360007).

References

1. L Wang, L. Mei, X. Liu, J. Shi, Y. Li, N. Gu, R. Cui, *Microchim. Acta*, 182 (2015) 1661.
2. H. Yang, Y. Li, Y. Liu, Y. Zhang, Y. Zhao, M. Zhao, *J. Solid State Electrochem.*, 19 (2014) 145.
3. M. Noroozifar, M. Khorasani-Motlagh, M. B. Parizi, R. Akbari, *Ionics*, 19 (2013) 1317.
4. Y.-H. Li., Y. Ji, B.-B. Ren, L.-N. Jia, Q. Cai, X.-S. Liu, *J. Iran. Chem. Soc.*, 16 (2019) 1903.
5. X.-D. Xiao, L. Shi, L.-H. Guo, J.-W. Wang, X. Zhang, *Spectrochim. Acta A*, 173 (2017) 6.
6. X, Liu., W, Zhang., L, Huang. N. Hu, W. Liu, Y. Liu, S. Li, C. Yang, Y. Suo, J. Wang, *Microchim. Acta*, 185 (2018) 234.
7. F.-e Lin, C. Gui, W. Wen, T. Bao, X. Zhang, S. Wang, *Talanta*, 158 (2016) 292.
8. Y. Li., H, W. Peng, X. You, *Microchim. Acta*, 184 (2017) 3539.
9. W. Gao, L. Qi, Z. Liu, S. Majeed, S. A. Kitte, G. Xu, *Sensor. Actuat. B-Chem.*, 238 (2017) 468.
10. J. Lee, J. Son, H.Y. Koh, A. N. Pae, D.-H. Kim, *Anal. Biochem.*, 313 (2003) 292.
11. V. V. Tolmacheva, D. I. Yarykin., M. V. Gorbunova, V. V. Apyari, S.G. Dmitrienko, Y. A. Zolotov, *J. Anal. Chem.*, 74 (2019) 1057.
12. S, Palanisamy., X. Zhang, T. He, *Sci. China Chem.*, 59 (2016) 387.
13. Z. Yang, Y. Zhu, M. Chi, C. Wang, Y. Wei, X. Lu, *J. Colloid Interf. Sci.*, 511 (2018) 383.

14. H. Ye, H. Wang, B. Zhang, F. Zhao, B. Zeng, *Talanta*, 186 (2018) 459.
15. J. Peng, W. Zhuge, Y. Liu, C. Zhang, W. Yang, Y. Huang, *J. Electrochem. Soc.*, 166 (2019) B1612.
16. J. Pillay, K. I. Ozoemena, *Electrochim. Acta*, 52 (2007) 3630.
17. B. S. Jilani, C. D. Mruthyunjayachari, P. Malathesh, Mounesh, T. M. Sharankumar, K. R. Venugopala Reddy, *Sensor. Actuat. B-Chem.*, 301 (2019) 127078.
18. J. Peng, W. Zhuge, Y. Huang, C. Zhang, W. Huang, *B. Korean Chem. Soc.*, 40 (2019) 214.
19. W. Zhuge, X. Li, S. Feng, *Microchem. J.*, 155 (2020) 104726.
20. J. Peng, Q. Huang, W. Zhuge, Y. Liu, C. Zhang, W. Yang, G. Xiang, *Biosens. Bioelectron.*, 106 (2018) 212.
21. J. Peng, Q. Huang, Y. Liu, P. Liu, C. Zhang, *Sensor. Actuat. B-Chem.*, 294 (2019) 157.
22. J. Peng, Q. Huang, Y. Liu, Y. Huang, C. Zhang, G. Xiang, *Electroanal.*, 32 (2020), Early Access, DOI: 10.1002/elan.201900505.
23. Y. Zhang, W. Hu, *Sci. China Ser. B.*, 52 (2009), 751.
24. R. Koeppe, A. Fuchsbauer, S. Lu, N. S. Sariciftci, *Progr Colloid Polym Sci.*, 135(2008) 16.
25. S. Riyazi. M. E. Azim Araghi. *J. Mater. Sci.-Mater. El.*, 31 (2020) 3539.
26. J. P. F. Longo, S. C. Leal, A. R. Simioni, M. de F. M. Almeida-Santos, A. C. Tedesco, R. B. Azevedo, *Laser. Med. Sci.*, 27 (2012) 575.
27. Y. Gök, H. Z. Gök, M. K. Yılmaz, M. Farsak, İ. ÜmitKarayiğit, *Polyhedron*, 153 (2018), 128.
28. Y. Chen, M. Hanack, W. J. Blau, D. Dini, Y. Liu, Y. Lin, J. Bai, *J. Mater. Sci.*, 41 (2006) 2169.
29. Z. Biyiklioglu, O. Bekircan, *Synthetic Met.*, 200 (2015) 148.
30. Y. Gök, H. Z. Gök, İ. Ü. Karayiğit, *J. Organomet. Chem.*, 873 (2018) 43.
31. Y. Li , X. Liu, X. Zeng, X. Liu, B. Kong, W. Wei, S, Luo, *Electrochim. Acta*, 56 (2011) 2730.
32. S. Chaiyo, E. Mehmeti, W. Siangproh, T. L. Hoang, H. P. Nguyen, O. Chailapakul, K. Kalcher, *Biosens. Bioelectron.*, 102 (2018) 113.
33. K. Kunpatee, P. Chamsai, E. Mehmeti, D. M. Stankovic. A. Ortner, K. Kalcher, A. Samphao, *J. Electroanal. Chem.*, 855 (2019) 113630.
34. J. Feng, X. Wang, S. Han, X. Ji, C. Li, C. Luo, M. Sun, *Microchim. Acta*, 186 (2019) 769.
35. S. Hu, H. Zhu, S. Liu, J. Xiang, L. Zhang, *Microchim. Acta*, 178 (2012) 211.
36. G. R. Chaudhary, S. Bansal, P. Saharan, P. Bansal, S. K. Mehta, *BioNanoScience*, 3 (2013)241.
37. S. Chaiyo, E. Mehmeti, W. Siangproh, T.i L. Hoang, H. P. Nguyen, O. Chailapakul, K. Kalcher, *Biosens. Bioelectron.*, 102 (2018) 113.
38. Y. Peng, Z. R. Tang, Y. P. Dong, G Che, Z. Xin, *J. Electroanal. Chem*., 816 (2018) 38.
39. D. Jia, L. Wang, Y. Gao, L. Zou, B.Ye, *J Electroanal. Chem.*, 764 (2016) 56.
40. Q. Huang, X. Li, S. Feng, W. Zhuge, F. Liu, J. Peng, Shancai Mo, *Anal. Methods-UK*, 10 (2018) 3594.
41. X. Dong, M. Li, N. Feng, Y. Sun, Z. Xu, C. Yang, RSC Adv., 5 (2015) 86485.
42. S. K. Arumugasamy, S. Govindaraju, K. Yun, *Appl. Surf. Sci.*, 508 (2020) 145.
43. S. Lu, M. Hummel, K. Chen, Y. Zhou, S. Kang, Z. Gu, *Electrochem. Commun.*, 114 (2020) 106715.
44. S. B. Matt, S. Manjunatha, S. Manjunatha, D. M. Sidlingappa, M. Sidlingappa, ChemistrySelect, 2019 (4) 5839.
45. W. Zhang, G. Jia, Z. Li, C. Yuan, Y. Bai, D. Fu, *Adv. Mater. Interfaces*, 4 (2017) 1601241.
46. S. Z. Bas, C. Cummins, A. Selkirk, D. Borah, M. Ozmen, M.l A. Morris, *ACS Appl. Nano Mater.*, 2 (2019) 7311.
47. P. Pang, F. Yan, H. Li, H. Li, Y. Zhang, H. Wang, Z. Wu, W. Yang, *Anal. Methods-UK*, 8 (2016) 4912.
48. H. Xu, J. Xiao, L. Yan, L. Zhu, B. Li, *J. Electroanal. Chem.,* 779 (2016) 92.